Location Study of Solar Thermal Power Plant in the State of Bahia using Geographic Information Systems (GIS) and Economic Methods

Chigueru Tiba and Verônica Wilma B. Azevêdo

[1] Universidade Federal de Pernambuco, Centro de Tecnologias e Geociências, Departamento de Energia Nuclear, Recife, Pernambuco (Brazil)

Abstract

Solar Thermal Technology for the generation of electricity in large scale has been a reality in the world since the 1980s, when the SEGS plants were introduced. Nine SEGS power plants were built in three different sites in the Mojave Desert, in California (USA), between 1984 and 1991, and still in commercial operation today, with 354 MW of installed capacity, demonstrating their technical and commercial reliability. In Brazil, this form of energy generation has not yet been explored for large scale projects. In order to contribute for the introduction of solar thermal technology in Brazil, in large scale projects, this paper presents a study of the optimal location for thermoelectric power plants, based on the cost of electricity generation. The applied methodology for Bahia, located in the Northeast Region of Brazil, considered the implantation of parabolic trough solar power plant of 80MWe, operating only in solar mode, without heat storage. Based on performed analysis, it was confirmed that Bahia presents great potential for the installation of solar power plants, especially in the west region of State.

Keywords: Solar Thermal Technology, Large-Sized Solar Plants, GIS, Bahia, Brazil.

1. Introduction

Brazil has a mainly renewable energy matrix, with greater participation of water (66.6%), biomass (8.5%), wind (7.6%) and solar photovoltaic (0.5) resources (BEN, 2019). However, although it shows a remarkably renewable character, it is notable that the generation of electricity by solar thermal technology, in large scale projects (above 80 MW), remains unexplored.

To contribute for the introduction of solar thermal technology in Brazil, this paper presents a study of the optimal location for thermoelectric power plants, based on the cost of electricity generation. For a solar thermal power plant hypothetically located at a pixel set, the cost of electric energy generated was calculated considering the capital cost, the electric energy generated and the infrastructural costs (high tension grid and additional pipelines). The methodology applied for Bahia, Northeast region of Brazil, considered the implantation of parabolic through solar power plants of 80 MW, SEGS type, operating only in solar mode, without heat storage. The solar power plant with nominal power of 80 MW.

2. Solar Thermal Power Plant

2.1. Solar Technology

According to Dahle et al. (2008) the concentrating solar power plants produce electric power by converting the sun's energy into high-temperature heat using various mirror configurations. The heat is then channeled through a conventional generator. The plants consist of two parts: one part collects solar energy and converts it to heat, and the other converts heat energy to electricity.

In parabolic trough systems, the sun's energy is concentrated by parabolically curved, trough-shaped reflectors onto a receiver pipe running along the inside of the curved surface. This energy heats oil flowing through the pipe, and the heat energy is then used to generate electricity in a conventional steam generator.

Selection and/or peer review under responsibility of Scientific Committee
doi:10.18086/swc.2019.18.01 Available at http://proceedings.ises.org

2.2. Solar Field Modeling for Parabolic Collectors

According to Broesamle et al. (2001) the electric energy generated by a parabolic trough solar power plant, may be determined by a mathematical function which considers thermal energy generated by the power plant, the nominal efficiency of the steam cycle and the parasitic losses.

To simulate the thermal energy generated by a solar plant of 80MW, SEGS type, which uses the parabolic collectors energy, it was used a simplified and stationary model of the physical properties of the parabolic LS-3 collector of SEGS. In this model, the geometrical, optical and thermal losses were modeled. Concerning geometrical losses, the following effects are considered:

a) The cosine effect (ξ_{cos}): for a horizontally aligned collector and parallel to the north-south axis is given by the following equation:

$$\xi_{\cos\theta} = \sqrt{\cos^2\theta_z + \cos^2\delta \ \sin^2\omega} \qquad \text{(eq. 1)}$$

Where: θ = incidence angle; θ_z = Zenith angle; δ = declination angle; ω = time angle.

b) Losses related to the incidence angle modifier (ξ_{IAM}): that considers the reflected image distortion due to the non-perpendicular incidence of the radiation. According to Patnode (2016) the modifier of the incidence angle can be given by the following expression:

$$K = \cos(\theta) + 0.000884(\theta) - 0.00005369(\theta^2) \quad \text{(eq. 2)}$$

For Patnode (2006) it is important to distinguish the existing losses in the solar radiation available due to the incidence angles corrections (empirical) of absorption and reflection correlated to the incidence angle. Therefore, it is necessary to divide the incidence angle modifier by the cosine of the incidence angle, as shown in the following equations (eq. 3 and eq. 4):

$$\xi_{IAM} = \frac{K}{\cos(\theta)} \qquad \text{(eq. 3)}$$

$$\xi_{IAM} = 1 + 0.000884\frac{\theta}{\cos(\theta)} - 0.00005369\frac{\theta^2}{\cos(\theta)} \qquad \text{(eq. 4)}$$

c) Collector end loss factor (ξ_E): that comprehends the solar light fraction that is reflected by the collector and does not illuminate a certain length of the absorbing tube. The losses in the ends of the collectors are given in function of the focal length of the collector, the length of the solar collector and the incidence angle, and are given by:

$$\xi_E = 1 - \frac{f\tan(\theta)}{L_{SCA}} \qquad \text{(eq. 5)}$$

Where: f = focal length of the collectors; L_{SCA} = length of the solar collector.

d) Losses related to shading (ξ_S): The shading in the solar field decreases the performance of the collectors once it attenuates the collection of solar radiation. According to [18], the shading factor in the columns is defined by:

$$\xi_S = \frac{W_{eff}}{W} = \frac{L_{spacing}}{W}.\frac{\cos\theta_z}{\cos\theta} \qquad \text{(eq. 6)}$$

Where: W_{eff} = opening effective width of the collector; $L_{spacing}$ = length of the space between the columns (15m for the SEGS VI); W = opening width of the collector (5m for the LS-2 collectors); θ_z = Zenith angle.

With all the effects defined, the geometrical losses of the system may be determined by the following equation:

$$\xi_{geo} = \xi_{IAM}.\xi_S.\xi_E.\xi_{COS} \qquad \text{(eq. 7)}$$

The second group of losses considers the optical losses of the collector, which come from the reflection, transmission and non-ideal absorption of solar radiation. For model simplification purposes, all the coefficients that define optical losses were considered constant. As a matter of fact, its values may vary, for example, the reflectivity of the mirrors that may present different values due to the cleaning actions performed on them. All the coefficients considered in the simulation, and its respective medium values, are presented in Table 1.

Tab. 1: Coefficients Considered for the Determination of Optical Losses

Coefficient	Symbol-Value	Explanation
Reflection of the Mirrors	ε_T – 0.93	Losses due to the reflection once not all the incident radiation is reflected.
Dirt on the mirrors	ϑ – 0.98	Dirt on the surface of the mirrors, which reduce the reflection.
Transmittance of the Mirrors	μ – 0.99	Losses related to coverage of the mirrors that absorb a portion of the incident radiation.
Interception Factor	ρ_m – 0.90	Related to the mirrors manufacture.
Transmittance factor of the tube, which involves the absorber tube	σ_T – 0.95	Due to the coverage of the glass that protects the absorber and prevents the transmittance of all the radiation.
Absorption coefficient of the absorber tube	τ – 0.95	Due to the portion of radiation that is reflected by the absorber tube.

Once all the coefficients are constants, the optical efficiency of the collector in the solar field is given by (Richts, 2012):

$$\eta_{opt} = \varepsilon_T \, \vartheta \, \mu \, \rho_m \, \sigma_T \, \tau = 0.7329 \quad \text{(eq. 8)}$$

The third group of losses considers the instantaneous thermal losses of the solar field, to which are related with the difference of temperature of the absorber tube's surface (T_A = 653K) and the ambient temperature perceived by the absorber tube when exposed to sun light. Such loss is given by the following expression:

$$\dot{q}_{loss} = A_{SF} \, . \, \left[(b_1 \, \Delta T + b_2 \Delta T^2) + \dot{q}_{pipeloss} \right] \quad \text{(eq. 9)}$$

Where: $\dot{q}_{loss}$ = instantaneous thermal losses in the solar field; A_{SF} = solar field area; b1 and b2 = coefficients empirically determined for the collector of Euro Trough II equipped with the PTR70 absorber tube and worth, respectively, 0 W/m²K and 0.00047 W/m²K² (Riffelmann, 2005); ΔT = temperature difference between the absorber tube and the ambient temperature; $\dot{q}_{pipeloss}$ = instantaneous additional losses existing on the pipes of the solar field.

From the modeling of the losses related to the solar collectors and with the knowledge of the direct normal irradiation incident and the area of the solar field, it is possible to define the instantaneous thermal energy generated in the power plant through the following equations:

$$\dot{Q}_{SF} = \dot{Q}_{in} - \dot{Q}_{loss} \quad \text{(eq. 10)}$$

$$\dot{Q}_{in} = A_{SF} \, . \, DNI \, . \, \varepsilon_{geo} \, . \, \eta_{opt} \quad \text{(eq. 11)}$$

$$\dot{Q}_{loss} = \int_{dia} \dot{q}_{loss} \, dt = 12 \, \dot{q}_{loss} \quad \text{(eq. 12)}$$

Where: $\dot{Q}_{SF}$ = instantaneous thermal energy in the solar field; $\dot{Q}_{in}$ = instantaneous potency absorbed; $\dot{Q}_{loss}$ = daily thermal losses of the solar field; A_{SF} = solar field area; DNI = direct normal irradiation; ξ_{geo} = geometric efficiency; η_{opt} = optical efficiency; $\dot{q}_{loss}$ = the instantaneous thermal losses in the solar field.

In one year of operation, the thermal energy generated by the solar plant ($P_{net}^{Thermal}$) is given by:

$$P_{net}^{Thermal} = 365 \,.\, \dot{Q}_{SF} \qquad \text{(eq. 13)}$$

Finally, the electrical energy generated by the plant (E_{year}) can be described as:

$$E_{year} = P_{net}^{Thermal} \,.\, (\eta_{nom} - P_{Par,SF} - P_{Par,PB}) \qquad \text{(eq. 14)}$$

Where: η_{nom} = nominal efficiency of the power cycle; $P_{Par,SF}$ = parasitic electric consumption of the solar field; $P_{Par,PB}$ = parasitic electric consumption of the power cycle.

2.3. Economic Analysis

According to Broesamle et al. (2001), the LCOE generated by a plant that operates exclusively in solar mode is given by:

$$C_{el} = \frac{\frac{i\,.(1+i)^n}{(1+i)^n-1}.(I_{plant} + I_{inf}) + C_{O\&M}}{E_{year}} \qquad \text{(eq. 15)}$$

$$I_{inf} = \frac{C_{road}}{km} \,.\, d_{road} + \frac{C_{htg}}{km} \,.\, d_{dhtg} + \frac{C_p}{km} \,.\, d_p \qquad \text{(eq. 16)}$$

$$C_{O\&M} = C_{per} + 0.01 \,.\, (I_{plant} + I_{inf}) \qquad \text{(eq. 17)}$$

Where: i = rate of return of capital; n = life span; I_{plant} = investment cost; I_{inf} = total cost of infrastructure; $C_{O\&M}$ = annual costs with operation and maintenance; E_{year} = annual liquid energy generation; $C_{road/km}$ = cost, per kilometer, for the roadway interconnection; d_{road} = distance from the roadway; $C_{htg/km}$ = cost, per kilometer, for the electrical interconnection; d_{htg} = distance from the high tension grid; $C_{p/km}$ = cost, per kilometer, for the hydraulic interconnection; d_p = distance from hydraulic resources and C_{per} = cost with the workers.

3. Geographic Information Systems

According to Ribeiro (2005) GIS are computer systems developed with the purpose of digital processing of geographic information, considering its geometric, topological and temporal aspects. They are composed by software resources developed to enhance the acquisition of geographic data, research and spatial analysis of geographic phenomenon and facts, and also generate maps, letters, digital plants and various reports, reaching geographic information integration in several themed levels.

GIS can be represented as a net that links people to the spatial data, through the use of hardware, software and proceedings. The hardware correspond to the computing platform used; the software correspond to the programs and modules; the data represent the cartographic basis; the people represent the professionals responsible for the project as well as the users of the system; and finally, the proceedings comprehend the methodologies and the existing practical actions for the system to operate properly for the organization (Longley et al. 2005).

4. Methodology

4.1. Material Used

The material used included: Softwares ArcGIS 10.1 (ESRI) and Spring 5.2.6 (INPE), Shapefiles of the study

area, Mission data SRTM3, Satellite images LANDSAT 8, Sun Positions Algorithm (SOLPOS) and Meteorological Database for Teaching and Research (BDMEP).

4.2. Study Area

According to IBGE (Brazilian Institute of Geography and Statistics), Bahia is located in the Northeast Region of Brazil, between the coordinates 18.348560º and 8.532821º South Latitude and -37.341147º and -46.617097º West Longitude.

4.3. Methodological Procedures

The steps taken for the definition of potential sites are presented in the flowchart in Figure 1.

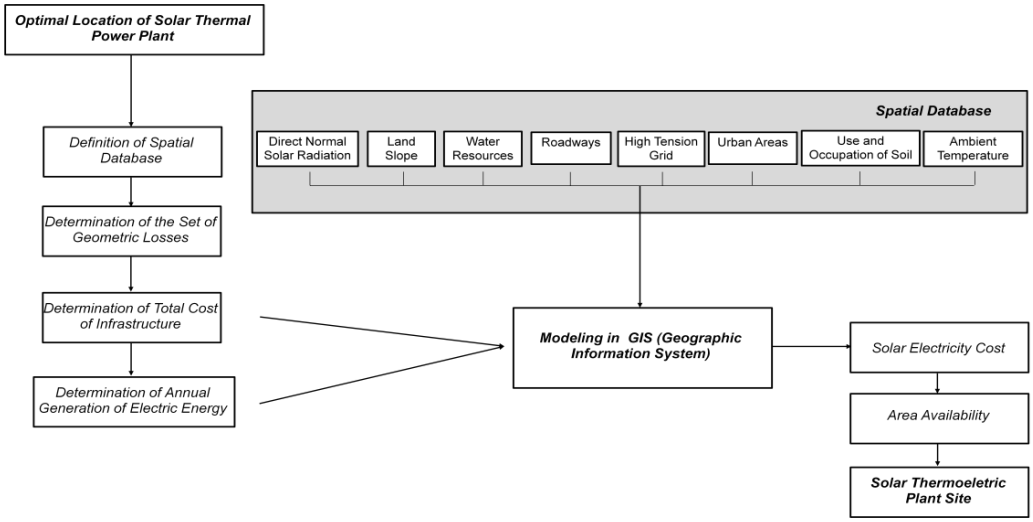

Fig. 1: Flowchart of the methodology.

a) Definition of Spatial Database: The Spatial Database, or simply BDE, gathers properly updated spatial information of the territory with a view to actions for planning, management and development of projects effectively and sustainably (Alcântara and Sá, 2011).

For the study of optimal location of solar thermal power plants in Bahia, the BDE structuring of the BDE followed the construction process since the Cartographic Basis already exist and are available for application. The steps followed for the construction of this BDE involved actions of surveying, analyzing and systematizing existing information, quality analysis of spatial data, base edition and preparation of the database. The spatial data that contributed to the BDE were direct normal irradiation, land slope, water resources, roadways, high tension grid, urban areas, use and occupation of soil and ambient temperature.

The spatial data of direct normal irradiation (annual average daily value) in Bahia are distributed in 10km x 10km cells and expressed in kWh/m² - SWERA (2018). The solar radiation rates vary from 3.8 to 6.3kWh/m². The highest values (between 5.9 and 6.3kWh/m²) are located in the Barreiras, Juazeiro, Irecê e Guanambi. The lowest values observed (between 3.8 and 4.3kWh/m²) are prevalent in Feira de Santana, Salvador, Santo Antônio de Jesus, Ilhéus-Itabuna e Vitória da Conquista.

b) Determination of the Set of Geometric Losses: to define the values of the losses related to shading (η_{shadow}), to collector ends ($\eta_{endloss}$) and to the incidence angle modifier (K), first, for the State of Bahia, seventeen municipalities well distributed throughout the State, were chosen for representation in the model. After the selection of the municipalities, the survey of meteorological information necessary for the implementation of the model was performed.

The meteorological variables of atmospheric pressure and dry-bulb temperature acting in the region of each municipality researched in the Meteorological Database for Teaching and Research (BDMEP), of National Institute of Meteorology INMET. The BDMEP is a database to support teaching and research activities and other applications in meteorology, hydrology, water resources, public health, environment, etc. The database gathers daily meteorological data, in digital form, of historical series from Conventional Meteorological

Stations of INMET network, according with the International Technical Standards of the Word Meteorological Organization.

The atmospheric pressure data corresponded to the monthly average values obtained throughout the year of 2017 in each municipality. Therefore, the annual average value in each locality was calculated from these monthly values. On the other hand, the dry-bulb temperature data obtained refer to daily and hourly determinations of 2017. Thus, for the implementation in the model, we sought to use the information regarding the Average Day of the Month, according Rabl (1965).

With all the data available, the next step was the determination of the position of the Sun in each locality. Each step was performed with the aid of SOLPOS. SOLPOS is an algorithm developed by NREL (National Renewable Energy Laboratory) which determines, among others, the position of the Sun for a given locality in function of localization and time. It is available in the Internet and its information is considered valid for the determinations performed between the years of 1950 and 2050, with an uncertainty of ± 0.01 degrees.

In SOLPOS were inserted the information of geographic localization, atmospheric pressure, dry-bulb temperature and Coordinated Universal Time (UTC) for each municipality. As algorithm output data, the monthly average values obtained were the hourly, zenithal and solar declination angles. From these, the calculation of the parameters regarding the losses related to shading (η_{shadow}), to collector ends ($\eta_{endloss}$) and to the incidence angle modifier (K) were performed, using the equations 1, 2, 4 and 5.

With the monthly average values of the losses related to shading (η_{shadow}), to collector ends ($\eta_{endloss}$) and to the incidence angle modifier (K) of each municipality used in the model, were calculated, then, the annual average values of these effects, which are presented in Table 2. Due to the similarity between the values found in the municipalities of Bahia, the value used to represent the effects of shading (η_{shadow}), of the final losses in the collector ends ($\eta_{endloss}$) and the incidence angle modifier (K) for the State of Bahia (annual average) was the average of the annual values of each one of these effects (which is also shown in Table 2).

Tab. 2: Annual Average Values of Losses to Shading (η_{shadow}), to Collector Ends ($\eta_{endloss}$) and to Incidence Angle Modifier (K)

Municipality	η_{shadow}	$\eta_{endloss}$	K
Barreiras	0.8709	0.9707	0.9943
Bom Jesus da Lapa	0.8817	0.9698	0.9935
Caetité	0.8884	0.9696	0.9927
Canavieiras	0.9139	0.9683	0.9911
Caravelas	0.9101	0.9669	0.9890
Cipó	0.9219	0.9711	0.9948
Correntina	0.8733	0.9702	0.9934
Feira de Santana	0.9170	0.9705	0.9940
Guaratinga	0.9089	0.9676	0.9901
Irecê	0.8940	0.9711	0.9947
Jaborandi	0.8643	0.9694	0.9925
Jacobina	0.9055	0.9712	0.9948
Lençóis	0.8973	0.9705	0.9938
Remanso	0.8926	0.9718	0.9957
Salvador	0.9197	0.9701	0.9934
Santa Rita de Cássia	0.8742	0.9712	0.9950
Vitória da Conquista	0.9005	0.9689	0.9919

Bahia (Annual Average)	**0.8961**	**0.9699**	**0.9932**

c) Determination of Total Cost of Infrastructure: To determine the total cost of infrastructure (I_{inf}), which relates the expenses to the electric, hydric and road interconnections of the power plant, were used the thematic layers relative to the distances to water resources, distance to main roadways and distances to high tension grids, as well as the parameters values $C_{htg/km}$ (cost, per kilometer, for the electrical interconnection through high tension grid) $C_{p/km}$ (cost, per kilometer, for the hydraulic interconnection) and $C_{road/km}$ (cost, per kilometer, for the road interconnection), shown in Table 3. All of these parameters were inserted in the GIS environment, according to the equation 16, to obtain the total cost of infrastructure (Azevedo, 2016). A schematic illustration of the total cost of infrastructure determination is presented in Figure 2.

Tab: 3 Fixed Parameters used for the location of the Solar Power Plant by LCOE.

Parameters	Value	Unit
I_{plant}	240,553,296.00	US$
I	8	%
n	25	Years
$C_{htg/km}$	334,101.80	US$/km
$C_{p/km}$	40,378.88	US$/km
$C_{road/km}$	50,115.27	US$/km
C_{per} – Cost with the workers	2,405,532.96	US$

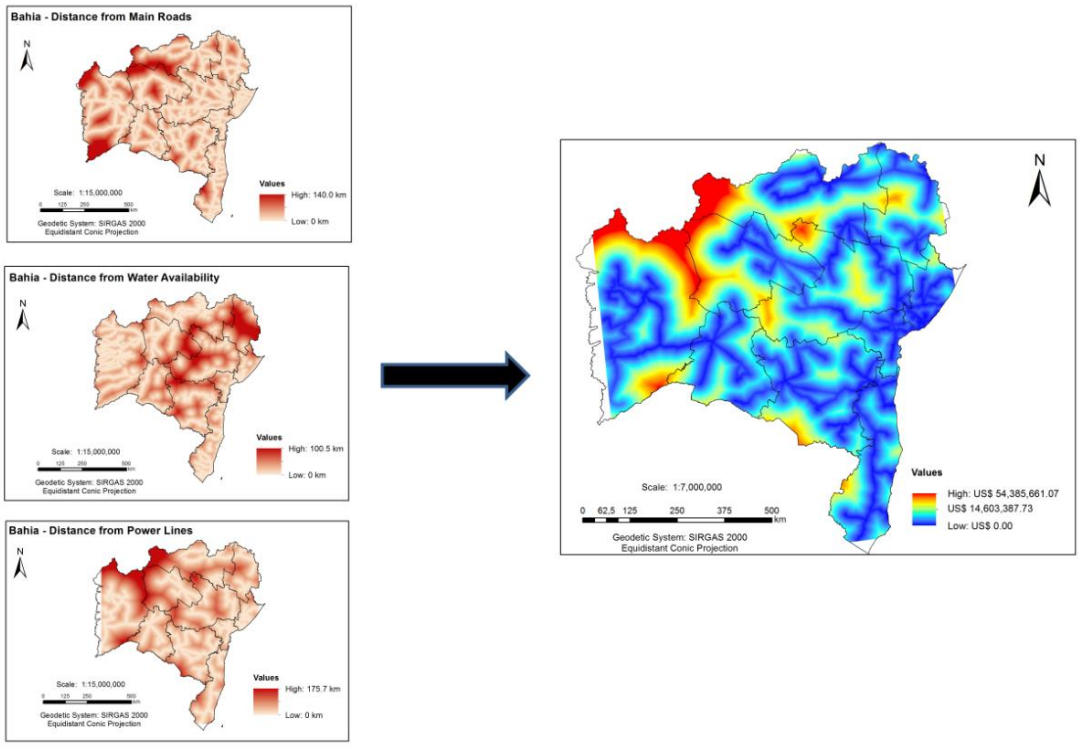

Fig. 2: Procedures for Calculation of the Infrastructure Costs.

d) Determination of Annual Generation of Electric Energy: The calculation of the amount of thermal energy generated in the solar field of the plant, hypothetically situated in the State of Bahia, succeeded the determination of the thermal energy absorbed and the definition of thermal losses.

For the determination of thermal energy absorbed, the equation 11 was used considering the use of the value obtained by Shenk and Eck (2012) to represent the maximum optical efficiency of the solar collector ($\eta_{opt,0}$ = 0.7330), the use of the constant 0.96 to represent the availability coefficients of the solar field (x_{field}) and cleaning of the mirrors (Cl), that is, ($Cl \cdot x_{field}$ = 0.96), the determination of the set of losses related to shading (η_{shadow} = 0.8961), to collector ends ($\eta_{endloss}$ = 0.9699) and to the incidence angle modifier (K= 0.9932) for Bahia, and the adoption of the value of 510,000m² for the representation of the total collector opening area in the solar field, that is, A_{SF} = 510,000m².

For the determination of thermal losses the equation 12 was used, considering the value used by Morin et al., (2012) for the representation of additional thermal losses existing in the solar field pipe ($q_{pipeloss}$ = 10W/m²), the value also used by Morin et al., (2012) for the fluid temperature at the inlet of the solar field ($T_{f,in}$ = 280ºC or 553K) and the fluid temperature at the outlet of the solar field ($T_{f,out}$ = 411ºC or 684K), the duration of 12 hours of operation of the plant for the calculation of thermal losses and the value of 510,000m² for the representation of the total opening area of the collectors in the solar field, that is, A_{SF} = 510,000m².

From the knowledge of all the parameters involved, it was possible to create a Map of Annual Production of Thermal Energy of a Solar Power Plant of 80MW for the State of Bahia, which is presented in the following section.

5. Results and Discussion

5.1 Costs of Electricity Production for Bahia

The costs of electric energy generation for Bahia are presented in Figure 3. In the map, it can be noticed that the highest costs (US$227.98/MWh) are located, mostly, in east part of Bahia. The lowest costs, which amount to US$ 145.16/MWh, are predominant in west portion of Bahia.

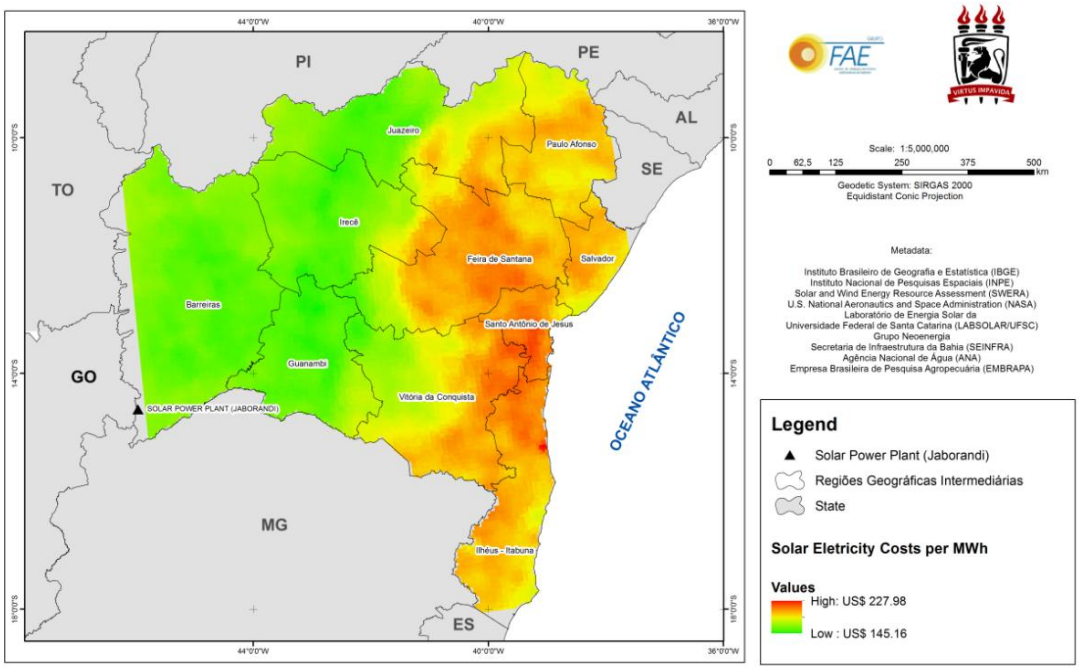

Fig. 3: Solar Electricity Costs Map per MWh of the Solar Thermal Power Plant of 80MW.

Observing the relation between the electric energy generation cost (C_{el}) and the annual energy generation (E_{year}) it is perceived that the sites with highest electric energy generation must present lower costs and vice-

versa, if all other factors are invariable. In fact, the highest values of E_{year}, which reach to 189400.5 MWh, are located in the west portion, where the costs by MWh reach US$ 145.16 (Figure 3 and Figure 4).

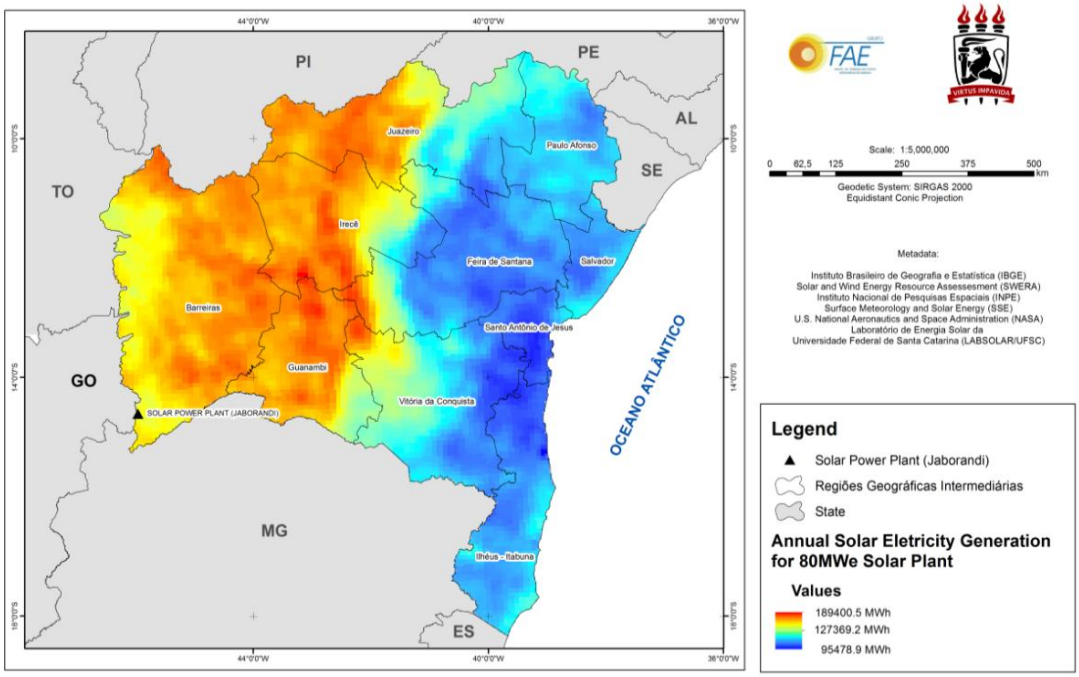

Fig. 4: Annual Solar Electricity Generation for 80MW Solar Plant.

Observing the relation between the LCOE and infrastructure cost (I_{inf}), it is verified that the higher the values of I_{inf} for a given value of energy production, the higher will be the LCOE. According to Figure 5, the regions that present higher I_{inf} (US$ 54,385,661.07) are located in the areas where there is low density of power grid.

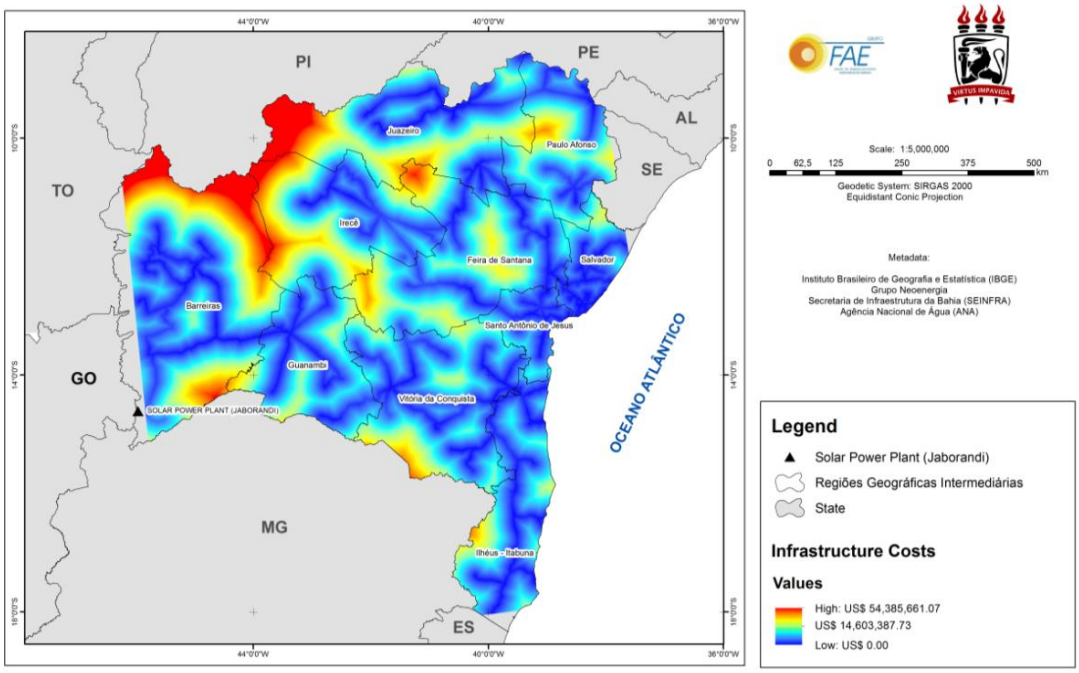

Fig. 5: Infrastructure Costs Map of the distances to roadways, high tension grids and water resources.

5.2 Identification of Promising Sites

To identify promising sites for solar plants installation in Bahia was made the identification of the restriction areas (Figure 6). The restriction areas considered in this study were (Tiba and Azevêdo, 2019): a) Federal Conservation Units; b) Indian territories; c) Quilombola territories; d) Atlantic Forest Remnants; e) High agricultural potential; f) Urban Areas; g) Water Bodies; and h) Sites with declivity higher than 5%.

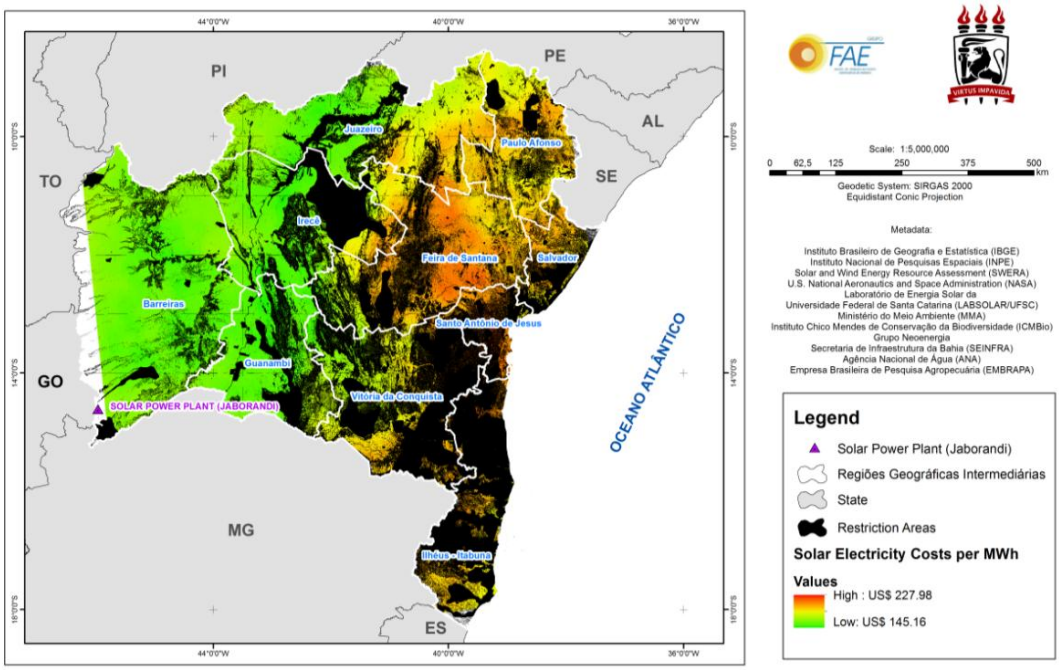

Fig. 6: Solar Electricity Costs Map per MWh and Restrictions Areas.

The total area availability for the installation is of 207,916.80km². Once determined the total area availability

for the installation, the best site determination was made, considering the lower electricity generation costs and the higher energy generation, as showed in Figure 7.

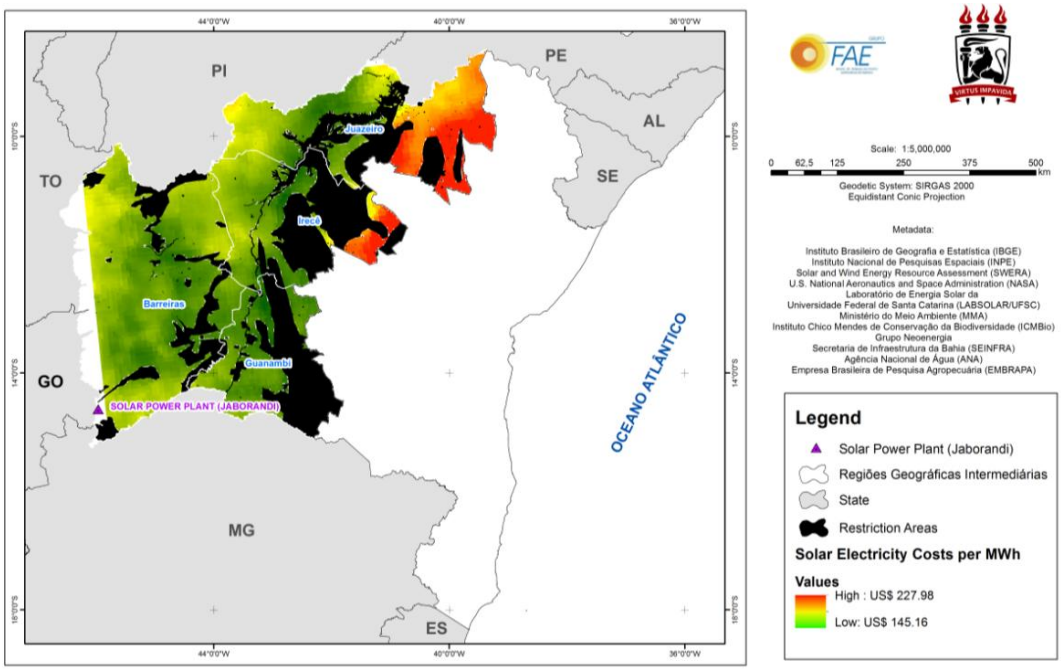

Fig. 7: The Best Sites for the Insertion of CSP Projects.

According to Figure 7, the regions of Barreiras, Guanambi, Irecê and Juazeiro, present great potential for the installation of CSP projects. In these regions it is possible to find areas with electric energy generation costs of US$ 145.16/MWh and values of energy production of 189,400.5MWh/year. If the scenario presented by Murphy et. al. (2019) becomes concrete, there will be a reduction on the cost of electric energy in the USA and current cost in the year of 2030, that is to say, the order of US$ 0.05/kWh for Brazil.

The Jaborandi Solar Power Plant, located at the RGI of Barreira, is inserted in a region with large potential for the installation of CSP projects due to its proximity to infrastructural elements, high annual electric power production, smaller costs of energy production and area availability for projects insertion. (Tiba and Azevedo, 2019).

It is also worth mentioning that a more detailed analysis in the site of implementation of the solar power plant is indispensable. Such analysis should include the local measurement of the incident direct normal irradiation for at least five years, the precise and updated information availability of the infrastructure objects (electric, roadway and water) as well as a visit (in loco) to the sites indicated as promising for the solar technology insertion.

6. Acknowledgments

We thank the Conselho Nacional de Pesquisa (CNPq) Grant No. 302251-2017-0 and P&D, Desenvolvimento de Tecnologia Nacional de Geração Heliotérmica de Energia Elétrica, PD-ANEEL 2290-0051/2016, Termopernambuco S. A and Universidade Federal de Pernambuco, for supporting the solar energy research projects and providing the material means and the scientific environment for the execution of this research.

7. References

Alcântara, L. A.; Sá, L. A. C. M. Estruturação de Base de Dados Espaciais para Sistema de Geoinformação de Suporte à Gestão de Recursos Hídricos Subterrâneos na Região Metropolitana do Recife. In: XIX Simpósio Brasileiro de Recursos Hídricos. Maceió, 2011.

Azevêdo, V.W.B. Estudo de Localização de Usina Solar Termoelétrica no Estado de Pernambuco. Ph.D. Thesis, Federal University of Pernambuco, Recife, Brazil, 2016.

BEN - Balanço Energético Nacional 2019: Ano base 2018. Empresa de Pesquisa Energética - EPE. Rio de Janeiro.

Broesamle, H., Mannstein, H., Schillings, C., Trieb, F. Assessment of Solar Electricity Potentials in North Africa based on Satellite Data and a Geographic Information System. Solar Energy, v. 70, p. 1-12. 2001.

Dahle D.; Elliott, D.; Heimiller, D.; Mehos, M.; Robichaud, R.; Schwartz, M.; Stafford, B.; Walker, A. Assessing the Potential for Renewable Energy Development on DOE Legacy Management Lands. In: National Renewable Energy Laboratory (NREL). 2008.

Longley, P.A.; Goodchild, M.F.; Maguire, D.J.; Rhind, D.W. Geographical Information Systems and Science". John Wiley & Sons Ltd, Toronto. 2nd Edition, 2005.

Morin, G., Dersch, J., Platzer, W., Eck, M., Harbele, A.. Comparison of Linear Fresnel and Parabolic Trough Collector Power Plants. Solar Energy, v. 86, pp. 1-12. 2012.

Murphy, Caitlin, Yinong Sun, Wesley Cole, Galen Maclaurin, Craig Turchi, and Mark Mehos. The Potential Role of Concentrating Solar Power within the Context of DOE's 2030 Solar Cost Target. Golden, CO: National Renewable Energy Laboratory. NREL/TP-6A20-71912. 2019.

Patnode, A. M. Simulation and Performance Evaluation of Parabolic Trough Solar 638 Power Plants. Master of Science. 271 p. Mechanical Engineering. University of Wisconsin-639 Madison. Madison, United States. 2006.

Rabl, A., Active Solar Colletors and Their Applications. Oxford University Press. New York. 1985.

Ribeiro, G. P. Tecnologias Digitais de Geoprocessamento no Suporte à Análise Espaço-Temporal em Ambiente Costeiro. Niterói: UFFL, 2005. Tese (Doutorado em Planejamento e Ordenamento Territorial e Ambiental) – Universidade Federal Fluminense. Niterói, 2005.

Richts, C. A. Comparative Analysis of CSP and PV Utilization until 2020. Thesis 642 Faculty of Electrical Engineering and Computer Science, University of Kassel. 2012.

Riffelmann, K. J. Comparison between PTR70 and UVAC: Efficiency Tests, Thermal 645 Loss Measurements and Raytracing Experiments. In: BMU Status Seminar, Stuttgart, July 1, 2005. <www.solar-thermie.org/veranstaltungsarchiv/documents/2005-07-647 01/qualitaetssicherung.pdf>. 2005.

Shenck, H.; Eck, M. Yield Analysis for a Parabolic Trough Power Plants – A Basic Approach, Stuttgart. 2012.

SWERA. Solar and Wind Energy Resource Assessesment. <http://swera.unep.net>. Acesso em 10 janeiro de 2018.

Tiba, C., and Azevedo, V. W. B., (2019). Relatorio Técnico 01 a 06, Período: 18 de agosto 17 a 17 de fevereiro/19, Projeto Desenvolvimento de Tecnologia Nacional de Geração Heliotérmica de Energia Elétrica – Contrato ANEEL-PD-02290-0051/2016, Chamada N0 019/2016 ANEEL.